

Microscopic theory of intervalley scattering in GaAs: k dependence of deformation potentials and scattering rates

Cite as: Journal of Applied Physics **68**, 1682 (1990); <https://doi.org/10.1063/1.346622>

Submitted: 31 January 1990 . Accepted: 15 April 1990 . Published Online: 17 August 1998

Stefan Zollner, Sudha Gopalan, and Manuel Cardona



View Online



Export Citation

ARTICLES YOU MAY BE INTERESTED IN

[Intervalley deformation potentials and scattering rates in zinc blende semiconductors](#)

Applied Physics Letters **54**, 614 (1989); <https://doi.org/10.1063/1.100895>

[Band structure, deformation potentials, and carrier mobility in strained Si, Ge, and SiGe alloys](#)

Journal of Applied Physics **80**, 2234 (1996); <https://doi.org/10.1063/1.363052>

[Femtosecond intervalley scattering in GaAs](#)

Applied Physics Letters **53**, 2089 (1988); <https://doi.org/10.1063/1.100290>

Ultra High Performance SDD Detectors



See all our XRF Solutions

Microscopic theory of intervalley scattering in GaAs: k dependence of deformation potentials and scattering rates

Stefan Zollner, Sudha Gopalan, and Manuel Cardona
 Max-Planck-Institut für Festkörperforschung, Heisenbergstrasse 1, D-7000 Stuttgart 80,
 Federal Republic of Germany

(Received 31 January 1990; accepted for publication 15 April 1990)

The "rigid-pseudoion" model is applied to intervalley scattering processes in GaAs. The intervalley deformation potentials (IDPs) that we obtain at high-symmetry points are in good agreement with previous calculations. We find that the IDPs show a strong dependence on the wave vector of the intervalley phonon, therefore a numerical integration over the Brillouin zone (e.g., with the tetrahedron method) is necessary to obtain realistic scattering rates that can be compared with those obtained from experiments. We calculate the lifetimes of electrons at the L and X valleys as a function of temperature (L : 2.2 ± 0.5 ps; X : 130 ± 20 fs at room temperature) and discuss our results in comparison with recent ultrafast laser experiments and Monte Carlo simulations. Finally, the IDPs show an anisotropy that might be important when simulating electrical transport in hot-electron devices.

I. INTRODUCTION

Intervalley scattering (IVS) processes are important for a large number of semiconductor phenomena: they have been discussed as a possible mechanism of superconductivity in semiconducting¹ and metallic² phases of Si and Ge. The indirect absorption in Ge, Si, GaP,³ AlSb,⁴ or AlAs, or in GaAs or GaSb under pressure⁵ is assisted by intervalley phonons. In electrical measurements, electrons may display a negative differential resistance due to scattering to a valley with a different mass, which may lead to a peak in the drift velocity versus field curve^{6,7} and to microwave oscillations (Gunn effect).⁸ IVS also has to be considered when studying ballistic transport in hot-electron transistors^{9,10} or diffusion of hot carriers under high electric fields.¹¹ For low carrier concentrations and medium electron energies (below the fundamental gap, where impact ionization¹² is not possible), IVS seems to be the dominant¹³ energy loss mechanism (see Refs. 14 and 15 for the influence of carrier-carrier scattering at higher carrier densities). Recently, much attention has been paid to the initial relaxation of electrons after pulsed or cw optical excitation, where intervalley scattering processes are also important. Here, the carriers are probed with time-resolved luminescence,¹⁶ Raman scattering,¹⁷ time-resolved photoemission,¹⁸ hot-electron luminescence,¹⁹⁻²¹ four-wave mixing,²² far-infrared frequency mixing,²³ or induced transmission^{24,25} measurements. Finally, the temperature shifts (broadenings) of band gaps^{26,27} are mainly²⁸ due to virtual (real) intervalley transitions, that can be treated with the same formalism as the real transitions responsible for the Gunn effect.

Let us consider an electron with wave vector \mathbf{k} and energy $E_{\mathbf{k}}$ in the lowest conduction band (band index n) of a semiconductor with $E_{\Gamma} < E_L < E_X$ conduction-band ordering,²⁹ e.g., in GaAs. Even in a pure crystal the mobility of the electron is limited, because it can collide with the lattice and absorb or emit a phonon with wave vector \mathbf{q} , mode j , and

energy $\Omega_{\mathbf{q},j}$ (see Fig. 1). The scattered electron will have a wave vector $\mathbf{k}' = \mathbf{k} \pm \mathbf{q} + \mathbf{G}$, where \mathbf{G} is a reciprocal lattice vector. By convention, we choose \mathbf{G} such that \mathbf{q} is within the first Brillouin zone (BZ). \mathbf{G} may not be unique if \mathbf{q} is on the surface of the BZ. The plus sign stands for absorption, the minus sign for emission of a phonon. A scattering process with nonzero \mathbf{G} is called *umklapp* process, otherwise it is termed a *normal* process. If \mathbf{q} is small [to be specific, if $|\mathbf{q}| \leq 0.2(2\pi/a)$, which is about one third of the distance between Γ and L in the Brillouin zone when a is the lattice constant], the interaction is called an *intravalley* scattering process which we will not consider here, as long-range forces (Fröhlich interaction) are also important in ionic semiconductors and cannot be neglected. If \mathbf{q} is large, however, long-range forces are negligible. The scattered electron will find itself in a different equivalent or nonequivalent valley. Such *intervalley* scattering processes are the subject of this study.

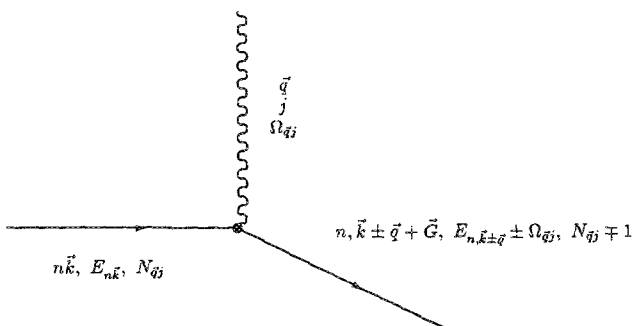


FIG. 1. An electron with wave vector \mathbf{k} , band index n , and energy $E_{n\mathbf{k}}$ interacts with the lattice and absorbs or emits a phonon with wave vector \mathbf{q} , mode j , and energy $\Omega_{\mathbf{q},j}$. The initial and final electron bands are assumed to be the same. The reciprocal lattice vector \mathbf{G} is chosen such that \mathbf{q} is within the first BZ. The number of phonons $N_{\mathbf{q},j}$ in the system is changed by 1. The lower sign stands for emission, the upper sign for absorption of a phonon.

In the past ten years, our group has been concerned with the systematic determination of the dependence of band gaps and broadenings on temperature.³⁰ The microscopic theory developed to describe such processes³¹ ("rigid-pseudoion" model) can easily be applied to other intervalley scattering processes. It is the purpose of this work to close the gap between our previous calculations and recent intervalley scattering experiments. We will follow the notation used previously as closely as possible and present the microscopic theory for intervalley scattering processes in Sec. II. We define the intervalley deformation potentials (IDPs) commonly used to interpret experiments in Sec. III, develop a scheme for calculating these deformation potentials, and present the results for IDPs between high-symmetry points. In Sec. IV we study the dependencies of these IDPs on the phonon wave vector. In Sec. V we show how these \mathbf{k} -dependent matrix elements can be integrated over the Brillouin zone to yield the temperature-independent intervalley phonon spectral function, from which the intervalley scattering rates can be obtained. In Sec. VI we describe the numerical procedure, present the results for lifetimes of electrons at the L and X point in GaAs as a function of temperature and compare these results with those obtained from recent ultrafast laser experiments. Finally, we summarize the results in Sec. VII.

There have been a few previous efforts to calculate IDPs: Cohen's group³² introduced the "rigid-pseudoion" model to calculate IDPs for IV-VI semiconductors in order to explain the superconductivity observed in these compounds. The model was later used for silicon^{33,34} and germanium.³⁵ Herbert performed the first calculation³⁶ of IDPs for zinc-blende semiconductors with a similar method. Recently, self-consistent pseudopotential calculations^{37,38} and an empirical tight-binding approach³⁹ were employed. None of these calculations, however, perform a detailed examination of the \mathbf{k} dependence of the IDPs necessary to calculate realistic energy-dependent scattering rates.⁴⁰ Detailed calculations of electron-phonon scattering demand at least a qualitative knowledge of the dependence of the IDP on \mathbf{k} . Processes are sometimes included which are forbidden at high symmetry points (e.g., $\mathbf{k} = 0$) by invoking that they become allowed for $\mathbf{k} \neq 0$. This can only be justified by a detailed analysis of the dependence of IDPs on \mathbf{k} .

The scattering times that we calculate in this work are for the limit of very low carrier densities. At higher densities, carrier-carrier scattering will change these rates, as final states may be occupied, in which case the Pauli principle will reduce the scattering rates. Therefore, the rates are density and even time dependent. Monte Carlo^{13,15} simulations will be necessary to compare the rates calculated from the microscopic theory (this work) with realistic experimental situations.

II. MICROSCOPIC THEORY

The rate $1/\tau_{qj}$ for the intervalley scattering process from a given valley as shown in Fig. 1 is given,⁴¹ to lowest order, by Fermi's "golden rule"^{42,43}:

$$\frac{1}{\tau_{qj}} = \frac{2\pi}{\hbar} |\langle n, \mathbf{k} \pm \mathbf{q}, N_{qj} \mp 1 | H_{\text{el-ph}} | n, \mathbf{k}, N_{qj} \rangle|^2 \times \delta(E_{n, \mathbf{k} \pm \mathbf{q}} \pm \Omega_{qj} - E_{n, \mathbf{k}}). \quad (1)$$

In this expression, $H_{\text{el-ph}}$ is the electron-phonon interaction Hamiltonian to be discussed below. $E_{n, \mathbf{k}}$ and $E_{n, \mathbf{k} \pm \mathbf{q}}$ are the electron energies before and after the scattering, respectively. In a first-order absorption process, the number of phonons N_{qj} in the system is decreased by one, while in an emission process it is increased by one. In thermal equilibrium with a lattice at temperature T , the phonon occupation number at a phonon energy Ω_{qj} is given by Bose-Einstein statistics

$$N_{qj} = [\exp(\Omega_{qj}/k_B T) - 1]^{-1}, \quad (2)$$

where k_B is the Boltzmann constant and j is the phonon branch index. In GaAs the band indices for the initial and scattered electron will be the same [unless the energies are extremely high, more than about 800 meV above the conduction-band (CB) edge]. We therefore use the same band index n for the initial and final electron states in Eq. (1) and in the forthcoming expressions in order to keep the notation simple. Sometimes processes with different band indices have to be considered, for example, in GaP, where an electron at Γ (Γ_1) may be scattered to the band at X with symmetry X_1 (same band) or X_3 (different⁴⁴ band). The extension of the notation to this case is straightforward.

In order to calculate the matrix element in Eq. (1), one has to know the electron and phonon states and their interaction Hamiltonian. The phonon energies Ω_{qj} have been measured with inelastic neutron scattering and are well known. Their dispersion can be calculated⁴⁵ with various semiempirical models (shell models,^{46,47} bond charge model,⁴⁸ etc.) or *ab initio* methods.^{49,50} The phonon eigenvectors also enter into the calculation. In principle, they are obtained by the models used, but the accuracy of these is questionable.^{51,52} (In Ref. 53 it was shown that seven different phonon models given seven very different sets of eigenvectors for the phonons at X and L in GaAs.) From the few experimental eigenvectors, derived at certain symmetry points for GaAs (Ref. 51) and Si,⁵⁴ and by comparison with *ab initio* calculations^{49,53,55,56} reasonable models can be chosen. The electronic energies and wave functions are obtained from band-structure calculations. In this work we use the empirical pseudopotential method^{57,58} (EPM) with a cutoff of about 5–7 Ry, corresponding to a basis set of 59–89 plane waves. The electron energies do not enter into the calculation of the matrix element, but are contained in the argument of the δ function. This justifies the work of Ref. 59, where the deformation potentials for non-energy-conserving processes between high-symmetry points are calculated.^{60–64} These deformation potentials contribute to the real and imaginary parts of the self-energy of electronic states.⁶⁵

The Hamiltonian for the interaction between the electron and the phonons is obtained from the electron-ion potential.³⁶ By Taylor-expanding this potential $V_\alpha(\mathbf{r} - \mathbf{R}_{l\alpha} - \mathbf{u}_{l\alpha})$ of an electron at position \mathbf{r} in the field of one ion of type α with basis vector τ_α in the unit cell at l that is currently displaced from its equilibrium position $\mathbf{R}_{l\alpha}$

$= I + \tau_\alpha$ by a phonon displacement $u_{i\alpha}$, we find the electron-phonon interaction Hamiltonian to lowest order in phonon displacement^{32,66}:

$$H_1 = - \sum_{i\alpha} u_{i\alpha} \cdot \text{grad } V_\alpha(\mathbf{r} - \mathbf{R}_{i\alpha}). \quad (3)$$

It is obvious that the interaction Hamiltonian does not act on the spin variables in this approximation. This has to be borne in mind when calculating scattering rates: the expression in Eq. (1) has to be integrated over all final states with the same spin as the initial state.

When calculating the matrix element entering the "golden rule" [Eq. (1)] using the interaction Hamiltonian of Eq. (3), we Fourier-transform the phonon displacement $u_{i\alpha}$ of the ion α to the normal mode representation.⁶⁷

$$u_{i\alpha} = \sum_{\mathbf{Q}j} \sqrt{\frac{\hbar^2}{2NM_\alpha\Omega_{\mathbf{Q}j}}} (a_{\mathbf{Q}j} + a_{\mathbf{Q}j}^\dagger) \epsilon(\mathbf{Q}j\alpha) \times \exp(i\mathbf{R}_{i\alpha} \cdot \mathbf{Q}). \quad (4)$$

Here N is the number of primitive cells, M_α the mass of an atom of type α (i.e., anion or cation), and $\epsilon(\mathbf{Q}j\alpha)$ is the normalized branch J phonon eigenvector of atom α . If we let the creation and annihilation operators $a_{\mathbf{Q}j}^\dagger$ and $a_{\mathbf{Q}j}$ act on the state $|N_{\mathbf{Q}j}\rangle$ and use Bloch's theorem in the form^{3,66}

$$\langle n, \mathbf{k} + \mathbf{q} | \text{grad } V_\alpha(\mathbf{r} - \mathbf{R}_{i\alpha}) | n, \mathbf{k} \rangle = \exp(-i\mathbf{q} \cdot \mathbf{l}) \langle n, \mathbf{k} + \mathbf{q} | \text{grad } V_\alpha(\mathbf{r} - \tau_\alpha) | n, \mathbf{k} \rangle, \quad (5)$$

we find the only nonzero matrix elements

$$\begin{aligned} \langle n, \mathbf{k} \pm \mathbf{q}, N_{\mathbf{Q}j} \mp 1 | H_1 | n, \mathbf{k}, N_{\mathbf{Q}j} \rangle \\ = \sum_{\alpha} \sqrt{\frac{\hbar^2}{2NM_\alpha\Omega_{\mathbf{Q}j}}} \mathbf{A}(\mathbf{k}, n, \pm \mathbf{q}, \alpha) \\ \cdot \epsilon(\pm \mathbf{q}j\alpha) \sqrt{N_{\mathbf{Q}j} + \frac{1}{2} \mp \frac{1}{2}}, \end{aligned} \quad (6)$$

where

$$\mathbf{A}(\mathbf{k}, n, \mathbf{q}, \alpha) = - \langle n, \mathbf{k} + \mathbf{q} | \text{grad } V_\alpha(\mathbf{r} - \tau_\alpha) | n, \mathbf{k} \rangle \exp(i\tau_\alpha \cdot \mathbf{q}). \quad (7)$$

In order to calculate the vector \mathbf{A} , we need to know the electron states and the gradient of the potential. This can be achieved by expanding the electron states into plane waves normalized over the primitive cell with volume V_0 :

$$|n, \mathbf{k}\rangle = \frac{1}{\sqrt{V_0}} \sum_{\mathbf{G}} C_{n\mathbf{k}}(\mathbf{G}) \exp[i(\mathbf{k} + \mathbf{G}) \cdot \mathbf{r}] \quad (8)$$

and Fourier-transforming the Cohen-Bergstresser⁵⁷ ionic potential (normalized⁵⁷ to the atomic volume $V_0/2$)

$$V_\alpha(\mathbf{g}) = \frac{2}{V_0} \int_{V_0} d^3\mathbf{r} V_\alpha(\mathbf{r}) \exp(-i\mathbf{g} \cdot \mathbf{r}), \quad (9)$$

which yields the potential in real space

$$V_\alpha(\mathbf{r}) = \frac{1}{2} \sum_{\mathbf{g}} V_\alpha(\mathbf{g}) \exp(i\mathbf{g} \cdot \mathbf{r}). \quad (10)$$

The sum in Eq. (8) runs over all reciprocal lattice vectors \mathbf{G} , that in Eq. (10), however, over the quasicontinuum of all vectors \mathbf{g} in reciprocal space, as the ionic potential $V_\alpha(\mathbf{r})$ is not periodic in the lattice.

After the plane-wave expansion of the electronic states and the ionic potential of Eq. (10) it is easy to calculate the gradient of the potential and to evaluate the matrix element defined in Eq. (6). The final result is³¹

$$\begin{aligned} \mathbf{A}(\mathbf{k}, n, \mathbf{q}, \alpha) \\ = - \frac{i}{2} \sum_{\mathbf{G}, \mathbf{G}'} C_{n, \mathbf{k} + \mathbf{q}}^*(\mathbf{G}') C_{n\mathbf{k}}(\mathbf{G}) (\mathbf{G}' - \mathbf{G} + \mathbf{q}) \\ \times V_\alpha(\mathbf{G}' - \mathbf{G} + \mathbf{q}) \exp[-i(\mathbf{G}' - \mathbf{G}) \cdot \tau_\alpha]. \end{aligned} \quad (11)$$

We approximate the crystal potential $V(\mathbf{g})$ in Eq. (11) with an interpolation of the pseudopotential form factors used in the band-structure calculation in a similar fashion as in Ref. 31. Sham⁶⁸ has shown that the use of a pseudopotential and pseudo-wave functions gives the same results when calculating electron-phonon matrix elements as the use of the real potential and real wave functions. This implies that $V_\alpha(|\mathbf{g}|)$ has to be known as a continuous function of $g = |\mathbf{g}|$ from $g = 0$ to a typical cutoff of about $g = 8\pi/a$, not just for the few reciprocal lattice vectors needed to calculate the band structure. The major drawback of the empirical pseudopotential method is, however, that the form factors are ill defined for small and large wave vectors g . For small g , two somewhat arbitrary extrapolations have been used: (i) screened ion limit for metals (our choice), which is similar to the Heine-Abarenkov-Animalu model potential,⁶⁹ and (ii) extrapolation to $V = 0$ for $g = 0$ (Bednarek and Rössler).³⁴ The smallest value of g needed in the calculation is $g = |\mathbf{q}|$, which is quite large, as we are mainly concerned with zone-boundary phonons. The other problem is whether or not one should cut off the pseudopotential at a certain g value (e.g., $g = \sqrt{11} * 2\pi/a$). We agree with Bednarek and Rössler³⁴ that the uncertainty in the electron-phonon matrix elements for the conduction band of silicon is about 20–30% for different extrapolations with the exception of the LA mode, for which the disagreement is larger. Unfortunately, there are no experimental data for this mode. For GaAs, the difference between the two extrapolations is also about 20%, but the same uncertainty appears when using different sets of pseudopotential form factors $V_\alpha(\mathbf{G})$, e.g., from Refs. 57 and 58. In this work, we always choose the screened-ion limit and set our form factors to zero for $g > \sqrt{11} * 2\pi/a$. The same sets of form factors were used for the calculation of the band energies and the electron-phonon matrix elements of Eq. (5). The results thus obtained agree reasonably with experiments.⁴⁰

These results can be used to calculate the intervalley scattering time defined in Eq. (1). We obtain

$$\frac{1}{\tau_{\mathbf{q}j}} = \frac{1}{\hbar} \frac{\partial \Gamma_{n\mathbf{k}}}{\partial N_{\mathbf{Q}j}} \times \begin{cases} N_{\mathbf{Q}j} & \text{for absorption} \\ N_{\mathbf{Q}j} + 1 & \text{for emission,} \end{cases} \quad (12)$$

where the electron-phonon coefficient

$$\begin{aligned} \frac{\partial \Gamma_{n\mathbf{k}}}{\partial N_{\mathbf{Q}j}} = \frac{\hbar^2 \pi}{N \Omega_{\mathbf{Q}j}} \left| \sum_{\alpha} M_\alpha^{-1/2} \mathbf{A}(\mathbf{k}, n, \pm \mathbf{q}, \alpha) \cdot \epsilon(\pm \mathbf{q}j\alpha) \right|^2 \\ \times \delta(E_{n, \mathbf{k} \pm \mathbf{q}} \pm \Omega_{\mathbf{Q}j} - E_{n\mathbf{k}}) \end{aligned} \quad (13)$$

is a special case of that in Refs. 70 and 31 and has the dimensions of an energy. It should not change by more than 10% between 0 and 400 K, as the phonon frequencies and band

energies depend only weakly on temperature. Therefore, most of the temperature dependence of the scattering time is contained in the phonon occupation factors N_{qj} . In Eq. (13) the plus sign stands for phonon absorption, whereas the minus sign stands for phonon emission. The sum runs over the atoms of the basis.

III. DEFORMATION POTENTIALS

The electron-phonon matrix elements introduced in Eq. (1) and experimental intervalley scattering rates for the conduction band (band index n) are often expressed in terms of the intervalley deformation potentials D . These are defined in the literature^{39,42,43,71-73} as

$$|\langle \mathbf{k} \pm \mathbf{q}, N_{qj} \mp 1 | H_{\text{el-ph}} | \mathbf{k}, N_{qj} \rangle| = \sqrt{\frac{\hbar^2}{2V\rho\Omega_{qj}}} D(\mathbf{q}, j, \mathbf{k}) \sqrt{N_{qj} + \frac{1}{2} \mp \frac{1}{2}}, \quad (14)$$

where V and ρ are the volume and the density of the crystal. This reduces to Conwell's approximation⁷¹ for the intervalley scattering time for a carrier with energy E to a set of equivalent final valleys (N_V is the number of such valleys) with mass m when D is assumed to be independent of the phonon mode ($\mathbf{q}j$) and the rate in Eq. (1) is just summed over all \mathbf{q} states allowed by the conservation of energy and spin. This is equivalent to multiplying the rate in Eq. (1) with the density of final states at energy E and with the same spin:

$$g(E)V = (N_V m^{3/2} V \sqrt{E}) / (\sqrt{2\pi^2 \hbar^3}). \quad (15)$$

Sometimes⁷¹ $D_i K$ or the \mathbf{q} -dependent formulation³² $q\zeta$ are used instead of D , but this is just a matter of notation. There is another more serious ambiguity, however, in the definition of D . Obviously the mass of the crystal $V\rho$ equals NM with N being the number of primitive cells, if $M = M_1 + M_2$ is the total mass in the primitive cell. This may seem awkward for the case of germanium or silicon, as

M has to be chosen to be twice the atomic mass, but it is the only definition consistent with that in the older literature,⁷¹ which arose as a generalization of the expression for long wavelength acoustic phonons (hence ρ). Cohen's group has used the more natural convention $M = (M_1 + M_2)/2$ in their calculation of intervalley deformation potentials for silicon³⁷ and some IV-VI compounds³² with rocksalt structure. The mentioned ambiguity arises from the attempt to write the matrix element as⁷⁴ $|\langle H_{\text{el-ph}} \rangle|^2 = D^2 u_{qj}^2$, u_{qj}^2 being a mean-squared vibrational amplitude

$$u_{qj}^2 = (\hbar^2/2NM\Omega_{qj})(N_{qj} + \frac{1}{2} \pm \frac{1}{2}) \quad (16)$$

For a monatomic lattice, there is only one natural choice for M , i.e., the atomic mass. In the zinc-blende structure, however, three possible choices are in use; for an optical phonon at $\mathbf{q} = 0$, the reduced mass is the natural choice.⁷⁴ The Conwell notation uses the mass of the primitive cell $M = M_1 + M_2$, but Cohen's notation (M is the mean mass) is equally attractive, as it reduces to the atomic mass for the diamond structure. We adopt the Conwell notation of $M = M_1 + M_2$ in all calculations in this work.

The intervalley deformation potential $D(\mathbf{q}, j, \mathbf{k})$ for the conduction band, as defined in Eq. (14), depends on the initial state \mathbf{k} and on the intervalley phonon wave vector \mathbf{q} and mode j . Just like the electron-phonon coefficient in Eq. (13), the deformation potential is almost temperature independent. By comparison of Eqs. (14) and (6) we obtain

$$D(\mathbf{q}, j, \mathbf{k}) = \sqrt{M} \left| \sum_{\alpha} \mathbf{A}(\mathbf{k}, n, \mathbf{q}, \alpha) \cdot \boldsymbol{\epsilon}(\mathbf{q}, j, \alpha) M_{\alpha}^{-1/2} \right|. \quad (17)$$

In Ref. 59 we had presented the calculated values of such deformation potentials for scattering between the three valleys at Γ , X , and L in the lowest conduction bands of eight zinc-blende semiconductors. Due to an inconsistency of convention, the values given there are too high by a factor of $\sqrt{2}$. We therefore list the corrected values for the intervalley deformation potentials in Table I and compare with other cal-

TABLE I. Calculated intervalley deformation potentials in units of eV/Å (corrected version of Table I in Ref. 59).

Material	$D_{\Gamma L}$			$D_{\Gamma X_1}$	$D_{\Gamma X_2}$	D_{LL}	$D_{X_1 X_2}$	D_{LX_1}			
	LA	LO	LA + LO ^a	LA/LO ^b	LA/LO ^c	LA + LO ^a	LA/LO ^b	TA ^d	LA	LO	TO ^d
Ge This work	2.8	0	2.8	2.4	3.0	0.3	3.7	0.5	0.5	2.5	1.6
Ge Refs. 33,3	5.3	0	5.3
Ge This work ^e	1.2	0	1.2	0.6	2.8	0.7	2.0	0.5	0.4	1.2	1.4
GaP This work	0.8	0.7	1.1	1.1	0.8	0.6	3.0	0.4	0.7	1.6	0.7
GaAs This work	3.0	0.4	3.0	2.9	3.3	1.2	4.9	0.8	0.4	1.8	1.8
GaAs Ref. 39	2.1	2.4	3.2
GaAs Ref. 36	3.4	4.4,5.5
InP Ref. 36	2.9	2.6
...
InP Ref. 39	2.6
...
InP This work	1.4	1.8	2.3	1.6	2.6	0.9	3.1	0.7	0.5	2.8	1.2
InAs Ref. 39	2.8
InAs This work	1.7	1.0	2.0	2.2	2.0	1.1	2.5	0.6	0.6	1.9	1.1

^a When adding scattering contributions, the squares of the IDPs have to be added, i.e., $D_{LA+LO}^2 = D_{LA}^2 + D_{LO}^2$.

^b For the zinc-blende structure, the X_1 phonon is allowed (either LA or LO, anion at the origin). For diamond, the X_1 phonon is doubly degenerate and can be taken half even and half odd (Ref. 62). The even mode is allowed, the odd mode is forbidden.

^c The X_2 phonon is allowed for the zinc-blende structure (either LA or LO).

^d The transverse phonons are doubly degenerate at the X point. The intervalley deformation potentials are for each of the two phonons.

^e Extrapolation according to Ref. 34.

culations. Experimental data for the different deformation potentials scatter between 1 and 10 eV/Å,⁷⁵ but the evaluation of the IDPs from experiments is usually difficult and controversial, see the recent review in Ref. 76. Our results for silicon differ from those of Glembocki and Pollak³³ by a factor of 2, which may be due to an inconsistency in their normalization of the pseudopotential form factors [see Eq. (9)].

If one assumes that the intervalley deformation potential and the phonon energy do not change in the vicinity of a band minimum at Γ , L , or X , then Eq. (1) can be integrated

over all possible final states to give an average intervalley scattering time for an isotropic (parabolic or nonparabolic) final valley, as described by Conwell⁷¹ and other authors.⁴² These scattering rates can be used as input for Monte Carlo simulations of electrical or optical measurements. In this work, however, we shall use a different approach. First we show that the deformation potentials exhibit a considerable dependence on the phonon wave vector q . Then we perform an explicit integration in q space with the tetrahedron method for a special case, in order to obtain the averaged scattering rate.

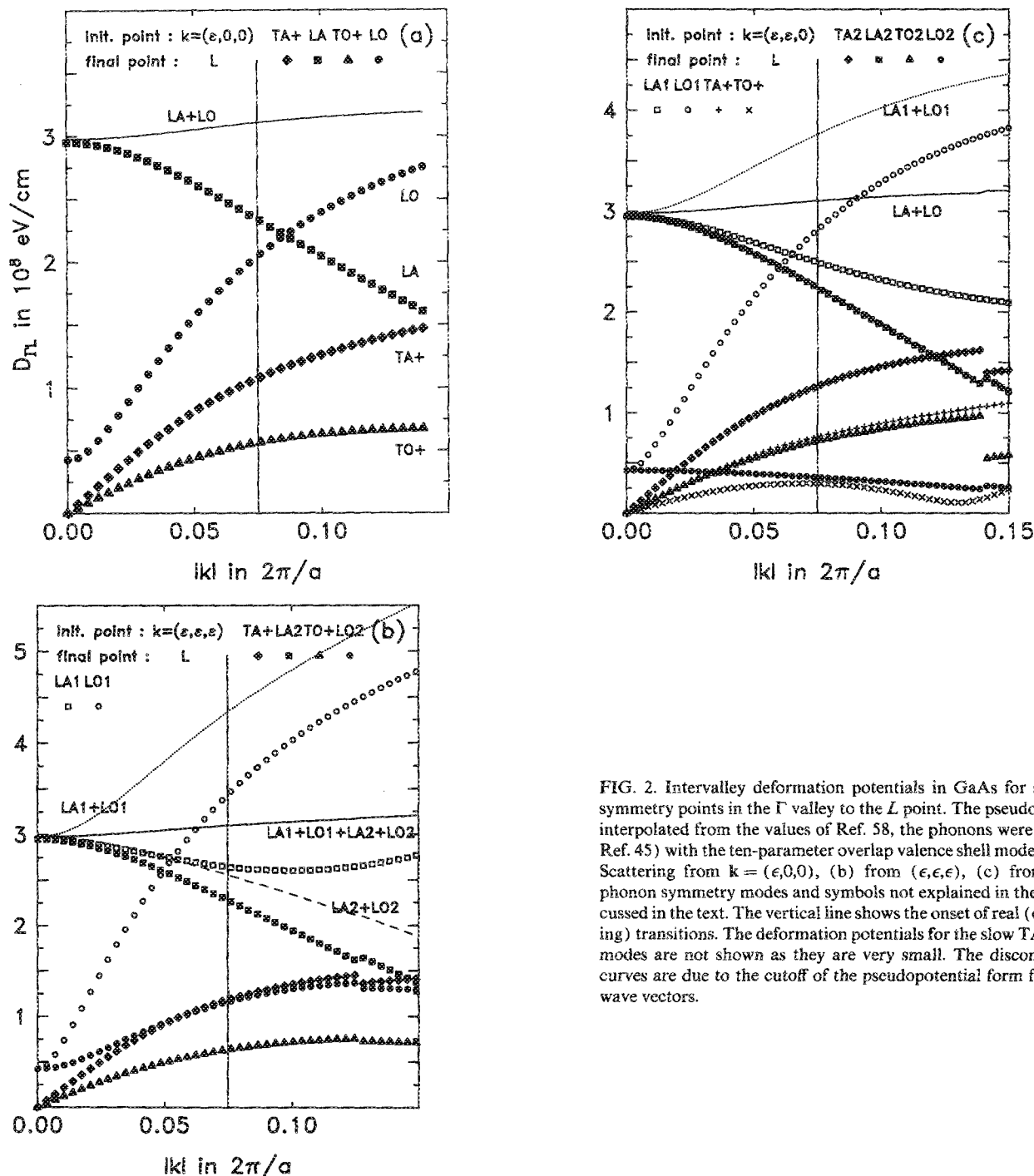


FIG. 2. Intervalley deformation potentials in GaAs for scattering from symmetry points in the Γ valley to the L point. The pseudopotentials were interpolated from the values of Ref. 58, the phonons were calculated (see Ref. 45) with the ten-parameter overlap valence shell model of Ref. 46. (a) Scattering from $k = (\epsilon, 0, 0)$, (b) from $(\epsilon, \epsilon, \epsilon)$, (c) from $(\epsilon, \epsilon, 0)$. The phonon symmetry modes and symbols not explained in the figures are discussed in the text. The vertical line shows the onset of real (energy-conserving) transitions. The deformation potentials for the slow TA and lower TO modes are not shown as they are very small. The discontinuities in the curves are due to the cutoff of the pseudopotential form factors for large wave vectors.

IV. k-DEPENDENCE OF INTERVALLEY DEFORMATION POTENTIALS

In Figs. 2 and 3 we show the deformation potentials in GaAs for scattering from points along (a) [100], (b) [111], and (c) [110] symmetry lines near the Γ point to the L or X points, respectively. (More precisely: from a point near Γ to points in the stars *L or *X). Along high-symmetry directions the phonon modes are slow (or lower) TA_s , fast (or upper) TA_f , LA, LO, lower TO_l , and upper TO_u . This notation is very intuitive, but not exact in off-symmetry directions as there is a considerable mixing between longitudinal and transverse phonons, especially between the longitudinal

and upper transverse ones. Table II shows the symmetries and selection rules of the intervalley phonons in the different directions. The upper two rows apply to this work (initial points in the stars *L and *X), the third row (initial point Γ , final point near X) is useful for the interpretation of Fig. 1 in Ref. 26.

First we discuss the scattering between *L and a point $k = (\epsilon, 0, 0)$ with ϵ small and positive. From now on, we state all coordinates in the Brillouin zone in multiples of $2\pi/a$. There are four *umklapp* and four normal processes possible, all having phonon wave vectors of the type $\mathbf{q} = (x, z, z)$ and a length of $|\mathbf{q}| = \frac{1}{2}\sqrt{3 - 4\epsilon}$, when the terms quadratic in ϵ are

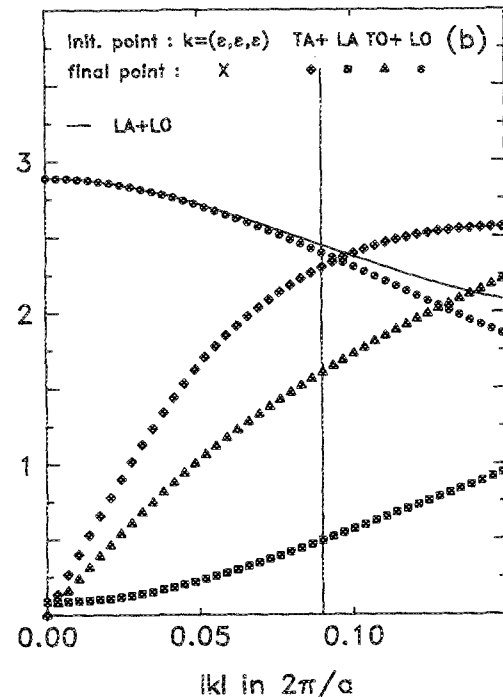
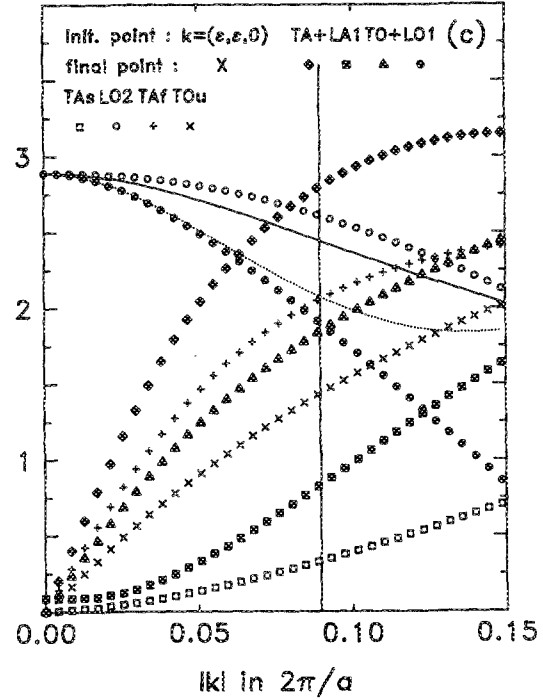
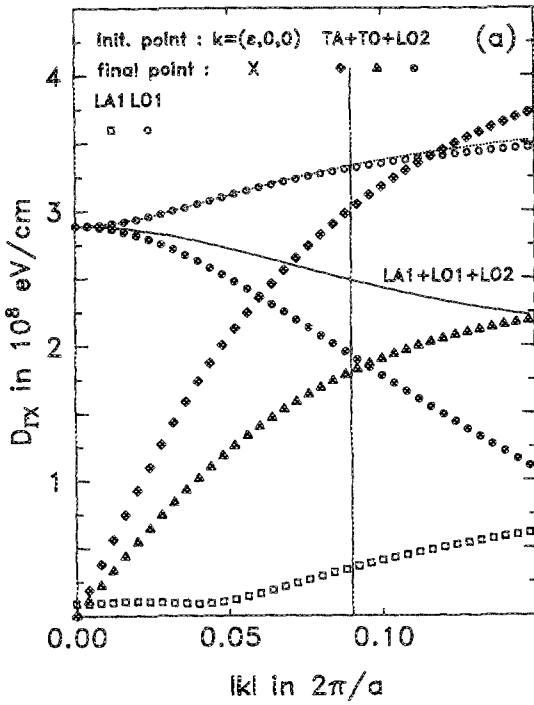


FIG. 3. As Fig. 2, but for the X point. The 14-parameter shell model of Ref. 47 was used in the calculation.

TABLE II. Symmetries for intervalley phonons in (100), (111), and (110) directions. The first two columns give the initial and final electron wave vectors, the third and fourth column the coordinates of the intervalley phonon and the square of its length to first order in ϵ (in units of $2\pi/a$, where a is the lattice constant). The column labelled "No." lists the total number of equivalent intervalley phonons with the same type of wave vector, the next column (U) only the *umklapp* processes. S means that the phonon wave vector is on the surface of the Brillouin zone, in which case normal and *umklapp* processes are the same. The last three columns give the symmetry of the intervalley phonon and the selection rules. C_2 stands for a reflection plane in the zincblende point group, $C_2(O_h)$ for a plane in the diamond group. (This symmetry is broken here by the lack of inversion symmetry, hence the selection rules are not exact.) Λ and Δ are the standard directions in the Brillouin zone. The first two wide rows (final points L and X) are relevant for the Figs. 2 and 3 of this work; the third row is useful when reading Fig. 1 of Ref. 26.

Final point k_f	Initial point k_i	Phonon q	Length $ q ^2$	No.	U	Symmetry	Allowed	Forbidden
*L	($\epsilon, 0, 0$)	($\frac{1}{2} - \epsilon, \frac{1}{2}$)	($3 - 4\epsilon$)/4	8	4	C_2	TA ⁺ , LA, TO ⁺ , LO	TA ⁻ , TO ⁻
	($\epsilon, \epsilon, \epsilon$)	($\frac{1}{2} - \epsilon, \frac{1}{2} - \epsilon, \frac{1}{2} - \epsilon$)	($3 - 12\epsilon$)/4	2	1	Λ	LA, LO	TA, TO
		($\frac{1}{2} + \epsilon, \frac{1}{2} - \epsilon, \frac{1}{2} - \epsilon$)	($3 - 4\epsilon$)/4	6	3	C_2	TA ⁻ , LA, TO ⁺ , LO	TA ⁻ , TO ⁻
	($\epsilon, \epsilon, 0$)	($\frac{1}{2}, \frac{1}{2} - \epsilon, \frac{1}{2} - \epsilon$)	($3 - 8\epsilon$)/4	4	2	C_2	TA ⁺ , LA, TO ⁺ , TO	TA ⁻ , TO ⁻
		($\frac{1}{2} - \epsilon, \frac{1}{2} + \epsilon, \frac{1}{2}$)	3/4	4	S	none	all	none
*X	($\epsilon, 0, 0$)	($1 - \epsilon, 0, 0$)	$1 - 2\epsilon$	2	1	Δ	LA, LO	TA, TO
		($1, \epsilon, 0$)	1	4	S	$C_2(O_h)$	TA ⁻ , LA, TO ⁺ , LO	TA ⁻ , TO ⁻
	($\epsilon, \epsilon, \epsilon$)	($1 - \epsilon, \epsilon, \epsilon$)	$1 - 2\epsilon$	6	3	C_2	TA ⁺ , LA, TO ⁺ , LO	TA ⁻ , TO ⁻
	($\epsilon, \epsilon, 0$)	($1, \epsilon, \epsilon$)	1	2	S	C_2	TA ⁺ , LA, TO ⁺ , LO	TA ⁻ , TO ⁻
		($1 - \epsilon, \epsilon, 0$)	$1 - 2\epsilon$	4	2	$C_2(O_h)$	TA ⁺ , LA, TO ⁺ , LO	TA ⁻ , TO ⁻
Initial point k_i	Final point k_f							
Γ	$X + *(\epsilon, 0, 0)$	($1 - \epsilon, 0, 0$)	$1 - 2\epsilon$	2	1	Δ	LA, LO	TA, TO
		($1, \epsilon, 0$)	1	4	S	$C_2(O_h)$	TA ⁺ , LA, TO ⁺ , LO	TA ⁻ , TO ⁻
	$X + *(\epsilon, \epsilon, \epsilon)$	($1 - \epsilon, \epsilon, \epsilon$)	$1 - 2\epsilon$	8	4	C_2	TA ⁺ , LA, LO ⁺ , TO	TA ⁻ , TO ⁻
	$X + *(\epsilon, \epsilon, 0)$	($1 - \epsilon, 0, 0$)	$1 - 2\epsilon$	8	4	$C_2(O_h)$	TA ⁺ , LA, TO ⁺ , LO	TA ⁻ , TO ⁻
		($1, \epsilon, \epsilon$)	1	4	S	C_2	TA ⁺ , LA, TO ⁺ , LO	TA ⁻ , TO ⁻
Γ	$L + *(\epsilon, 0, 0)$	($\frac{1}{2} - \epsilon, \frac{1}{2}$)	($3 - 4\epsilon$)/4	6	3	C_2	TA ⁺ , LA, LO, TO ⁺	TA ⁻ , TO ⁻
	$L + *(\epsilon, \epsilon, \epsilon)$	($\frac{1}{2} - \epsilon, \frac{1}{2} - \epsilon, \frac{1}{2} - \epsilon$)	($3 - 12\epsilon$)/4	2	1	Λ	LA, LO	TA, TO
		($\frac{1}{2} - \epsilon, \frac{1}{2} - \epsilon, \frac{1}{2} + \epsilon$)	($3 - 4\epsilon$)/4	6	3	C_2	TA ⁺ , LA, TO ⁺ , LO	TA ⁻ , TO ⁻
	$L + *(\epsilon, \epsilon, 0)$	($\frac{1}{2} - \epsilon, \frac{1}{2} - \epsilon, \frac{1}{2}$)	($3 - 8\epsilon$)/4	6	3	C_2	TA ⁺ , LA, TO ⁺ , LO	TA ⁻ , TO ⁻
		($\frac{1}{2} - \epsilon, \frac{1}{2} + \epsilon, \frac{1}{2}$)	3/4	6	S	none	all	none

neglected. The calculation shows that they all have the same deformation potentials. Here the slow TA and lower TO modes are odd with respect to the interchanging of two z coordinates (reflection in a plane) and therefore completely transverse. The other phonon modes are even with respect to that reflection and have mixed longitudinal and transverse character. As the electronic states in the lowest conduction band are even, only the even phonon modes contribute to intervalley scattering. It can be seen that the IDP of the LA mode [■ in Fig. 2(a)] rapidly decreases as $|k|$ increases, whereas the LO (●) contribution increases. This fact deserves some discussion: in germanium, where we have inversion symmetry, the LO phonon (L_1^+ symmetry in the diamond structure) cannot contribute to intervalley scattering between Γ (Γ_2^-) and L (L_1^+), whereas LA phonon (L_2^-) scattering is allowed. In GaAs or InSb this symmetry is broken only weakly: there should be some memory of the inversion symmetry of germanium. Therefore, one would expect the LA deformation potential to be larger than the LO IDP for small values of k , which is found in our calculations and in those for InP by Fawcett and Herbert.³⁶ It is important to note that the sum of the two processes [i.e., $\sqrt{D^2(\text{LA}) + D^2(\text{LO})}$], given by the line in Fig. 2(a), stays approximately constant. This sum is only meaningful if the

phonon energies of the LA and LO modes are about the same, which is roughly the case in GaAs. As can be expected, the two mainly transverse modes TA⁺ (◆) and TO⁺ (▲) gain importance as ϵ increases (see also Ref. 36). The importance of TA phonons has been observed in hot-electron luminescence experiments.⁷⁷

In Fig. 2(b) we show the results of a similar calculation for scattering between *L and a point $k = (\epsilon, \epsilon, \epsilon)$, with $\epsilon > 0$. Here we have to distinguish between two cases: (i) for scattering from (0.5, 0.5, 0.5) or (-0.5, -0.5, -0.5) to k [with q along the (111) direction, $|q| = \frac{1}{2}\sqrt{3 - 12\epsilon}$] the same symmetry rules as for scattering to the Γ point apply, and transverse phonons do not contribute. The IDPs for the longitudinal phonons, LA₁ (□) and LO₁ (○), are given by the open symbols, their sum by the dotted line. Discontinuities in the curves are due to the cutoff of the pseudopotential form factors at $2\pi\sqrt{11}/a$, as discussed above. (ii) The symmetry modes for scattering from the other six L points (across the zone, with $|q| = \frac{1}{2}\sqrt{3 - 4\epsilon}$) are TA⁺ (◆), LA₂ (■), TO⁺ (▲), and LO₂ (●), with (slow) TA⁻ and (lower) TO⁻ being forbidden [by parity, with respect to reflection in a (011) or equivalent plane, see Table II]. The IDPs for these modes are given by the closed symbols in Fig. 2(b). The sum of the LA₂ and LO₂ contributions is given by the

dashed line. The IDP for all longitudinal processes (i) and (ii), averaged over the star of L , is given by the solid line in Fig. 2(b), and it is approximately constant. This figure shows clearly that intervalley scattering is an anisotropic process, a fact which has to be taken into account in electrical transport measurements. Scattering processes with the same phonon wave vector contributing to different points in the same star have different IDPs [compare the open and closed circles in Fig. 2(b)].

The situation is more complicated for scattering between L and $\mathbf{k} = (\epsilon, \epsilon, 0)$; see Fig. 2(c). (i) There are four processes with $|\mathbf{q}| = \frac{1}{2}\sqrt{3} - 8\epsilon$, where LA_1 (\square), LO_1 (\circ), TA^+ ($+$), and TO^+ (\times) are allowed and TA^- and TO^- are forbidden. The sum of the LA_1 and LO_1 processes is given by the dotted line. (ii) For scattering from the other four L points, with $|\mathbf{q}| = \frac{1}{2}\sqrt{3}$, the symmetry restrictions are relaxed. Therefore, the lower TA_s and TO_l modes give small, but nearly negligible contributions ($D < 0.2$ eV/Å). The main processes are LA_2 (\blacksquare), LO_2 (\bullet) (mainly longitudinal), fast TA_2 (\blacklozenge), and upper TO_2 (\blacktriangle). The sum of LA_2 and LO_2 is given by the dashed line [almost hidden by the \blacksquare symbols in Fig. 2(c)], the average of all longitudinal processes under (i) and (ii) by the full line.

We summarize these results for $L\Gamma$ scattering as follows: the total intervalley deformation potential for longitudinal $L\Gamma$ scattering is about 3 eV/Å and almost independent of \mathbf{k} , when averaged over the star of L . The lower/slow transverse modes do not contribute to intervalley scattering, whereas the upper/fast modes contribute away from the center of the zone. Our calculation gives values for the latter of about 1 eV/Å for $|\mathbf{k}| = 0.07$, which is the \mathbf{k} vector for the onset of $L\Gamma$ scattering. The IDPs for *umklapp* and normal processes are identical; the relevant quantity seems to be the length $|\mathbf{q}|$ of the phonon wave vector.

We now proceed to discuss the scattering from one of the X points, beginning with the [100] direction. (i) For scattering to $\mathbf{k} = (\epsilon, 0, 0)$, there are two processes with $|\mathbf{q}| = 1 - \epsilon$, the corresponding symmetries being Δ_1 (LA and LO) and Δ_3 (TA and TO) (see Table II). For symmetry reasons, TA and TO scattering is forbidden, whereas LA_1 (\square) and LO_1 (\circ) are allowed. The calculation shows that LO_1 gives the main contribution, whereas the LA_1 IDP is small [see Fig. 3(a)]. The sum of the LA_1 and LO_1 processes is given by the dotted line. (ii) The other four processes have $|\mathbf{q}| = 1$. The TA^- and TO^- modes are not allowed for intervalley scattering in the diamond structure. The calculation shows that their IDPs are nearly zero for GaAs also. The LA_2 IDP also turns out to be small. The IDPs for TA^+ (\blacklozenge), LO_2 (\bullet), and TO^+ (\blacktriangle) are given in Fig. 3(a). It is worth noting that the TA^+ contribution is very large. This may explain the high rate for ΓX compared to ΓL scattering. The sum of all longitudinal processes, averaged over the star of X , is given by the full line. It slightly decreases with increasing $|\mathbf{k}|$, in good agreement with the overlap factor theory of Ref. 72.

The next case is scattering from a point in the star of X to $\mathbf{k} = (\epsilon, \epsilon, \epsilon)$. Naturally, all six processes have $|\mathbf{q}| = 1 - \epsilon$, with TA^- and TO^- forbidden, and TA^+ (\blacklozenge), LA (\blacksquare), TO^+ (\blacktriangle) and LO (\bullet) given in Fig. 3(b). The sum of all

longitudinal processes (LA and LO), given by the full line, slightly decreases away from the zone center. For scattering to a point $(\epsilon, \epsilon, 0)$, there are two processes with $|\mathbf{q}| = 1$. The IDPs for TA^+ (\blacklozenge), LA_1 (\blacksquare), TO^+ (\blacktriangle), and LO_1 (\bullet) are given in Fig. 3(c); the lower TA^- and TO^- modes are forbidden. The sum of LA_1 and LO_1 is given by the dotted line. For scattering from the other four X points, with $|\mathbf{q}| = 1 - \epsilon$, the contributions of the LA_2 and lower TO modes are small; those of slow TA_s (\square), fast TA_f ($+$), upper TO_u (\times), and LO_2 (\circ) are given in Fig. 3(c). The sum of all longitudinal processes (averaged over the star of X), given by the full line, slightly decreases.

We now summarize the main features of the \mathbf{k} dependence of the intervalley deformation potentials for scattering from the L or X point to a point \mathbf{k} in the Γ valley: (i) the total IDP for longitudinal phonons, when averaged over the star of L or X , is a nearly isotropic function of \mathbf{k} . It slightly decreases with increasing $|\mathbf{k}|$ for $X\Gamma$ scattering and stays almost constant for $L\Gamma$ scattering. This average is about the same for scattering from L and X . (ii) Nevertheless, intervalley scattering is highly anisotropic. Intervalley deformation potentials for scattering processes from the same \mathbf{k} point to different points in the same star may be different by almost an order of magnitude. (iii) Out of the four transverse phonon modes, the lower two modes can usually be neglected, whereas the upper two modes should always be taken into account. The fast TA_f mode for $X\Gamma$ scattering has a particularly high IDP. This may explain why ΓX scattering is seen to be stronger in experiments than ΓL scattering.

In order to investigate the anisotropy of the $L\Gamma$ IDPs even further, we write \mathbf{k} in spherical coordinates, keeping $|\mathbf{k}| = 0.07$ fixed, and vary the polar and azimuth angles in increments of 5° . Figure 4 shows such an angular dependence of the $L\Gamma$ IDPs in the x - y plane for scattering to $L = (0.5, 0.5, 0.5)$. The contribution of the lower/slow transverse phonon modes (not shown in the figure) never exceeded an IDP of 0.1 eV/Å. The upper TA mode increases from 0 up to 1.3 eV/Å, and the upper TO mode reaches a maximum of 0.7 eV/Å. Only the LO mode shows a strong anisot-

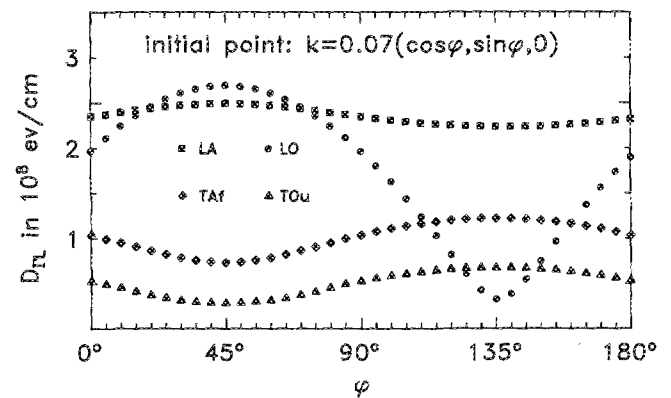


FIG. 4. Anisotropy of intervalley scattering: Deformation potentials for IVS from a point in the x - y plane of the BZ zone to the L point. Only the LO mode shows a strong anisotropy. The slow TA and lower TO modes give a very small contribution and are not displayed.

ropy, and the LA IDP stays approximately constant at about 2.2 eV/Å.

In a similar study of anisotropy for the X point, we keep $|\mathbf{k}|$ fixed at 0.09, which corresponds to the onset of ΓX scattering. The lower TA and TO modes stay relatively unimportant and never exceed an IDP of 0.6 eV/Å. The LA mode also gives very low values (up to 0.9 eV/Å), as can be expected from symmetry considerations. The dominant contributions come from the fast TA mode (IDP of 0–3.0 eV/Å), the LO mode (1.9–3.6 eV/Å), which is the one most favored by symmetry, and the upper TO mode (0–1.9 eV/Å). Figure 5 shows the anisotropy of ΓX scattering in the xy plane for scattering to $X = (1,0,0)$. Only one half of the plane is shown (Kramers degeneracy assumed).

This study shows that the intervalley deformation potentials display a considerable dependence on the wave vector of the intervalley phonon, but change smoothly over the Brillouin zone. Therefore, Conwell's formula⁷¹ will not be a good approximation. A linear interpolation and integration (e.g., with the tetrahedron method) is needed for an accurate estimate of intervalley scattering times. A mesh of 89 points in the irreducible wedge of the BZ (with 8 intervals along ΓX) will be too coarse in some cases, but one of 505 points (16 intervals along ΓX) should always be sufficient.

V. THE INTERVALLEY PHONON SPECTRAL FUNCTION

In order to find the average intervalley scattering time $\langle\tau\rangle$ for an electron at a given \mathbf{k} point (not the same for all wave vectors \mathbf{k} in a given valley!) to a different valley, one has to integrate Eq. (1) over all possible final states and sum up the contributions of all six phonon modes including the absorption and emission terms. The integration volume has to be chosen very carefully so as to include all final states in the desired valley, but to exclude intravalley and other intervalley scattering processes. Two special cases (initial \mathbf{k} points L and X) will be discussed below.

In order to separate the temperature dependent and independent parts of this integral, we introduce the dimensionless intervalley phonon spectral function⁷⁰

$$g^2 B(\mathbf{k}, \Omega) = \sum_j \int \frac{d^3 \mathbf{q}}{8\pi^3} \frac{\partial \Gamma_{\mathbf{k}}}{\partial N_{\mathbf{q}_j}} \delta(\Omega - \Omega_{\mathbf{q}_j}), \quad (18)$$

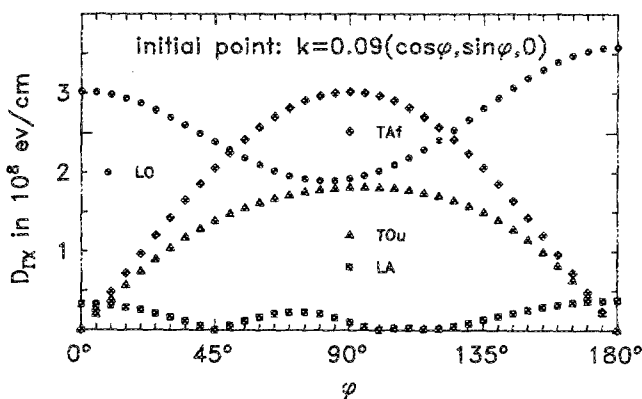


FIG. 5. As Fig. 4, but for the X point.

which corresponds to the density of phonon states weighted with the relevant intervalley deformation potential and the density of final electron states. If we neglect the small phonon energy term in the argument of the δ function in Eq. (13), the intervalley phonon spectral function is the same for both absorption and emission processes. Then the integrand in Eq. (18) is the same as in Refs. 70 and 31, but the volume of integration in \mathbf{q} -space has been constrained. The factor π in Eq. (16) of Ref. 70 is a misprint and should be deleted. We can write the averaged intervalley scattering time as a function of lattice temperature T as

$$\frac{1}{\langle\tau(T)\rangle} = \frac{2}{\hbar} \int_0^\infty d\Omega g^2 B(\mathbf{k}, \Omega) [N_\Omega(T) + \frac{1}{2}], \quad (19)$$

where N_Ω is the Bose-Einstein factor for the phonon energy Ω . Both emission and absorption processes are included (factor of 2 in front of the integral sign). The small temperature dependence of the electron and phonon energies have been neglected in this approximation.

It is obvious that Eq. (19) is substantially different from the isotropic approximation of Ref. 59. It does not contain a density of states mass as the integration is carried out numerically. If the intervalley phonon spectral function can be written as a δ function,

$$g^2 B(\mathbf{k}, \Omega) = \pi \hbar^2 / (\rho \Omega_{\text{eff}}) g(E_{\mathbf{k}}) D_{\text{eff}}^2 \delta(\Omega - \Omega_{\text{eff}}), \quad (20)$$

with an effective deformation potential D_{eff} , crystal density ρ , an electronic density of states $g(E_{\mathbf{k}}) = N_V m \sqrt{2m E_{\mathbf{k}}} / (2\pi^2 \hbar^3)$, and an effective phonon energy Ω_{eff} , then the constant terms can be taken out of the integral and the intervalley scattering time reduces to Conwell's approximation⁷¹:

$$\frac{1}{\langle\tau(T)\rangle} = \frac{2\pi \hbar}{\rho \Omega_{\text{eff}}} D_{\text{eff}}^2 g(E_{\mathbf{k}}) (N_{\text{eff}} + \frac{1}{2}), \quad (21)$$

where N_{eff} is the Bose-Einstein function with the argument Ω_{eff} .

VI. NUMERICAL PROCEDURE AND RESULTS

We have applied the theory explained above to calculate the intervalley phonon spectral function and the average return time for an electron at the L point to the Γ valley. The integration in Eq. (18) has to be performed over a spherical shell with a minimum radius of $0.2(2\pi/a)$ (to exclude intravalley scattering at L) and a maximum radius of $(\sqrt{3}/2) * (2\pi/a)$ to exclude L - L intervalley scattering. In the actual calculation with the tetrahedron method, the tetrahedra contributing to L - Γ scattering were chosen by inspection. We have also calculated the lifetime for an electron at the X point (X_1), which can scatter to the Γ valley or one of the four L valleys. Intravalley scattering at X and scattering to other X valleys was excluded. The electron states were calculated with empirical local pseudopotentials from Walter and Cohen⁵⁸ and a cutoff of 5–6 Ry, corresponding to 59–89 plane waves. For the phonons, a 10-parameter shell model⁴⁶ was used. Other pseudopotential form factors and phonon models gave similar results.

In order to calculate the intervalley phonon spectral function, one has to perform a summation over a part of the

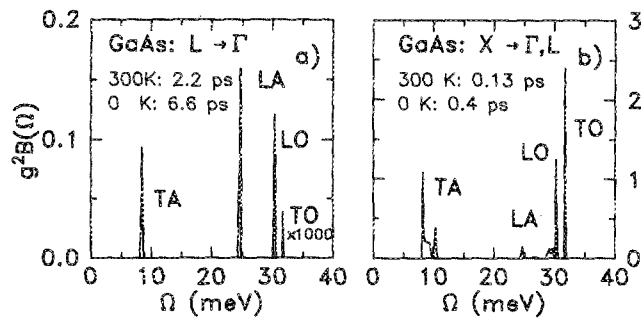


FIG. 6. Temperature-independent, dimensionless intervalley phonon spectral function $g^2B(\Omega)$ for the lifetime of an electron at the (a) L point and (b) X point. The abscissa is the energy of the intervalley phonon. This spectral function has to be multiplied with the Bose-Einstein factor and integrated over all phonon energies in order to obtain the lifetimes of the electrons as a function of temperature.

Brillouin zone with two δ functions. Such a summation is constrained to the intersection of two different constant-energy surfaces, one of which corresponds to electronic energy differences and the other to phonon energies. Allen⁷⁸ has generalized the tetrahedron method to such doubly constrained summations. Simple analytic results have been obtained by linearly interpolating the energies and matrix elements within a small tetrahedron. In the calculation, the irreducible $\frac{1}{48}$ th wedge of the BZ was divided into 1768 small tetrahedra which correspond to a mesh of 505 k points in the irreducible wedge (16 intervals along ΓX).

Figure 6(a) shows the intervalley spectral function for the return of an electron from the L point to the Γ valley. It can be seen that three phonons contribute to $L\Gamma$ scattering: the TA phonon ($\Omega = 8$ meV), the LA phonon (25 meV), and the LO phonon (30 meV). The contribution of the TO phonon (32 meV) is negligible [multiplied by 1000 in Fig. 6(a)]. This spectral function has to be integrated over all phonon energies [see Eq. (19)]. We obtain a return time of 6.6 ± 1 ps at low temperatures and 2.2 ± 0.5 ps at 300 K, in very good agreement with the results of Shah¹⁶ (2 ps at 300 K) and Alfano²² (2.7 ps). Figure 7(a) shows the $L\Gamma$ return time as a function of temperature.

We have also calculated the lifetime of an electron at the X_1 minimum in GaAs. Because of the higher density of states at the L points and the large deformation potentials for XL scattering,⁵⁹ electrons at X will mostly scatter to the L valleys (by emitting or absorbing an L phonon) rather than to the Γ valley (with an X phonon). In the L valleys they will rapidly relax to the minimum at or near L . From there they will finally scatter back to the Γ valley. The direct return from X to the Γ valley is also possible, but less probable. The

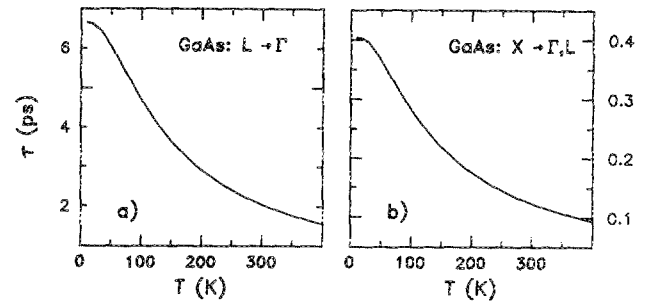


FIG. 7. Lifetimes (return times) of electrons at the (a) L and (b) X points as a function of temperature T , calculated from the pseudopotential form factors of Ref. 58 (with a cutoff of 6 Ry) and the shell model parameters of Ref. 46.

intervalley spectral function for an electron at X is shown in Fig. 6(b). The peaks can be identified with different phonon modes (see Table III). The contributions of the L phonons are generally larger than those of the X phonons as discussed above, with the exception of the LA(L) phonon that has a very small intervalley deformation potential.⁵⁹ We obtain a lifetime of 405 ± 90 fs (128 ± 20 fs) at 10 K (300 K) from the integrations, which is somewhat below the results of the recent infrared pump-and-probe experiment of Wang *et al.*⁷⁹ (700 ± 500 fs), but in good agreement with the Monte Carlo simulations of Kahn *et al.*¹⁵ The intervalley scattering time as a function of temperature is given in Fig. 7(b). The error for our calculation is much larger for the X point than for the L point, because our pseudopotential model for the conduction-band states is less reliable for higher energies.

VII. CONCLUSION

We have applied the "rigid-pseudoion" formalism to the calculation of intervalley deformation potentials for electrons in GaAs and other compound semiconductors. We have shown that the deformation potentials show a strong k dependence. Transverse phonons that are forbidden for scattering processes between high-symmetry points become allowed for the energy-conserving transitions observed in experiments. Especially the fast transverse acoustic mode should be considered when modeling hot-carrier experiments. In electrical measurements, where the applied electric field breaks the cubic symmetry, the anisotropy of the intervalley deformation potentials may become important, as the population of valleys parallel or perpendicular to the field will have different occupations.

Because of the k dependence of the deformation potentials, Conwell's scattering formalism is not a good approxi-

TABLE III. Intervalley phonons and their energies (from the 10-parameter valence overlap shell model of Ref. 46) for the spectral function of an electron at the X point

Phonon	TA(L)	TA(X)	LA(L)	LA(X)	LO(X)	LO(L)	TO(X)	TO(L)
Energy (meV)	8.1	9.6	25	27	29	30	31.1	31.7

mation to calculate intervalley scattering times. A numerical integration over the Brillouin zone (including details of the band structure and k -dependent matrix elements) should be performed, for example with the tetrahedron method. We have obtained an LT return time of 6.6 ps at 10 K (2.2 ps at 300 K) for GaAs. The lifetime of an electron at X_1 was found to be 400 fs at 10 K (130 fs at 300 K). Both numbers are in reasonable agreement with time-resolved luminescence and pump-and-probe experiments and Monte Carlo simulations with parameters obtained from an analysis of velocity-field curves. Further calculations of ΓL and ΓX scattering times in comparison with recent hot-electron luminescence measurements^{14,19-21} will be presented in a forthcoming publication.⁸⁰

It is difficult to apply the method to calculate scattering times for alloys (like AlGaAs) because the phonons are localized and k is no longer a good quantum number. A calculation for quantum wells or superlattices would require a supercell approach, which is very time consuming, but could be done in principle.

The method we have described is very fast and relatively easy to use. There are some disadvantages, however: the phonon states are calculated from parametrized models that are only heuristic fits to neutron scattering data and may not describe the phonon polarization vectors very well. *Ab initio* phonon calculations, on the other hand, are very time consuming or can only be used for special points, or both, and may not give correct phonon eigenvectors either. Another problem is the use of empirical pseudopotentials that may not give a good description of the conduction-band structure,⁸¹ but even most first-principles band-structure calculations (like the self-consistent pseudopotential method or LMTO) have to be adjusted in order to yield the correct band gap and dispersion of the conduction-band states. Nevertheless a first-principles calculation of intervalley deformation potentials should be performed at high-symmetry points in order to check the reliability of the "rigid-pseudopotential" method.

ACKNOWLEDGMENTS

The original program used in this study was written by P. Lautenschlager and P. B. Allen. We would like to thank K. Kunc, U. Rössler, and D. Strauch for valuable hints and discussions, and Chris Grein for a critical reading of the manuscript.

¹ M. L. Cohen, *Phys. Rev.* **134**, A511 (1964).

² K. J. Chang, M. M. Dacorogna, M. L. Cohen, J. M. Mignot, G. Chouteau, and G. Martinez, *Phys. Rev. Lett.* **54**, 2375 (1985).

³ F. H. Pollak and O. J. Glembocki, in *Electronic Structure, Dynamics, and Quantum Structural Properties of Condensed Matter*, edited by J. T. Devreese and P. Van Camp (Plenum, New York, 1985), p. 451 and references therein.

⁴ J. E. Rowe, M. Cardona, and K. L. Shaklee, *Solid State Commun.* **7**, 441 (1969); N. N. Sirota and A. I. Lukomskii, *Sov. Phys.—Semicond.* **7**, 140 (1973).

⁵ A. R. Goñi, K. Strössner, K. Syassen, and M. Cardona, *Phys. Rev. B* **36**, 1581 (1987).

⁶ M. A. Littlejohn, J. R. Hauser, and T. H. Glisson, *J. Appl. Phys.* **48**, 4587 (1977).

⁷ K. F. Brennan, D. H. Park, K. Hess, and M. A. Littlejohn, *J. Appl. Phys.* **63**, 5004 (1988).

⁸ J. B. Gunn, *Solid State Commun.* **1**, 88 (1963); *IBM J. Res. Dev.* **8**, 141 (1964); H. Kroemer, *Proc. IEEE* **52**, 1736 (1964).

⁹ M. Heiblum, E. Calleja, I. M. Anderson, W. P. Dumke, C. M. Knoedler, and L. Osterling, *Phys. Rev. Lett.* **56**, 2854 (1986).

¹⁰ K. Berthold, A. F. J. Levi, J. Walker, and R. L. Malik, *Appl. Phys. Lett.* **54**, 813 (1989).

¹¹ J. Vaitkus, A. Matulionis, L. Subacius, and K. Jarasiunas, in *19th International Conference on the Physics of Semiconductors*, edited by W. Zawadzki, (Institute of Physics, Polish Academy of Sciences, Warsaw, 1988), p. 1447.

¹² A. P. Dmitriev, M. P. Mikhaïlova, and I. N. Yassievich, *Sov. Phys. Semicond.* **17**, 28 (1983).

¹³ D. W. Bailey, C. J. Stanton, K. Hess, M. J. LaGasse, R. W. Schoenlein, and J. G. Fujimoto, *Solid-State Electron.* **32**, 1491 (1989); D. W. Bailey, C. J. Stanton, and K. Hess, *Phys. Rev. B* (in press).

¹⁴ J. A. Kash, R. G. Ulbrich, and J. C. Tsang, *Solid-State Electron.* **32**, 1277 (1989).

¹⁵ L. Rota and P. Lugli, *Solid-State Electron.* **32**, 1423 (1989); M. J. Kann, A. M. Krivan, and D. K. Ferry, *ibid.* **32**, 1831 (1989); SPIE Conf. Proc. **1282** (to be published); M. A. Osman and H. L. Grubin, *Phys. Rev. B* **40**, 1323 (1989); X. Zhou and T. Y. Hsiang, *J. Appl. Phys.* (in press).

¹⁶ J. Shah, B. Deveaud, T. C. Damen, W. T. Tsang, A. C. Gossard, and P. Lugli, *Phys. Rev. Lett.* **59**, 2222 (1987); D. Y. Oberli, J. Shah, and T. C. Damen, *Phys. Rev. B* **40**, 1323 (1989).

¹⁷ C. L. Collins and P. Y. Yu, *Phys. Rev. B* **27**, 2602 (1983); *ibid.* **30**, 4501 (1984); D. Kim and P. Y. Yu, *Phys. Rev. Lett.* **64**, 946 (1990).

¹⁸ R. Haight and J. A. Silberman, *Phys. Rev. Lett.* **62**, 815 (1989).

¹⁹ D. N. Mirlin, I. Ya. Karlik, L. P. Nikitin, I. I. Reshina, and V. F. Sapega, *Solid State Commun.* **37**, 757 (1981); D. N. Mirlin, I. Ya. Karlik, and V. F. Sapega, *ibid.* **65**, 171 (1988); M. A. Alekseev, I. Ya. Karlik, D. N. Mirlin, V. F. Sapega, and A. A. Sirenko, *19th International Conference on the Physics of Semiconductors* (Institute of Physics, Polish Academy of Sciences, Warsaw, 1988), Vol. 2, p. 1423.

²⁰ R. G. Ulbrich, J. A. Kash, and J. C. Tsang, *Phys. Rev. Lett.* **62**, 949 (1989).

²¹ W. Hackenberg, G. Fasol, H. P. Hughes, E. Bauser, and K. Ploog, *Solid State Electron.* **32**, 1247 (1989); G. Fasol, W. Hackenberg, H. P. Hughes, K. Ploog, E. Bauser, and H. Kano, *Phys. Rev. B* **41**, 1461 (1990).

²² A. Katz and R. R. Alfano, *Appl. Phys. Lett.* **53**, 1065 (1988).

²³ K. Kash, P. A. Wolff, and W. A. Bonner, *Appl. Phys. Lett.* **42**, 173 (1983); A. Mayer and F. Keilmann, *Phys. Rev. B* **33**, 6962 (1986).

²⁴ P. C. Becker, H. L. Fragnito, C. H. Brito Cruz, J. Shah, R. L. Fork, J. E. Cunningham, J. E. Henry, and C. V. Shank, *Appl. Phys. Lett.* **53**, 2089 (1988).

²⁵ R. W. Schoenlein, W. Z. Lin, E. P. Ippen, and J. G. Fujimoto, *Appl. Phys. Lett.* **51**, 1442 (1987); W. Z. Lin, R. W. Schoenlein, J. G. Fujimoto, and E. P. Ippen, *IEEE J. Quantum Electron.* **24**, 267 (1988).

²⁶ S. Zollner, J. Kircher, S. Gopalan, and M. Cardona, *Solid-State Electron.* **32**, 1585 (1989).

²⁷ W. W. Rühle, K. Leo, and E. Bauser, in *19th International Conference on the Physics of Semiconductors*, edited by W. Zawadzki, (Institute of Physics, Polish Academy of Sciences, Warsaw, 1988), p. 1399.

²⁸ Apart from a trivial thermal expansion term, which is usually much smaller, see Ref. 31.

²⁹ D. E. Aspnes, C. G. Olson, and D. W. Lynch, *Phys. Rev. Lett.* **37**, 766 (1976); D. E. Aspnes, *Phys. Rev. B* **14**, 5331 (1976).

³⁰ For a recent review see M. Cardona and S. Gopalan, in *Progress on Electron Properties of Solids*, edited by R. Girlanda (Kluwer, Dordrecht, The Netherlands, 1989), p. 51.

³¹ C. K. Kim, P. Lautenschlager, and M. Cardona, *Solid State Commun.* **59**, 797 (1986); S. Gopalan, P. Lautenschlager, and M. Cardona, *Phys. Rev. B* **35**, 5577 (1987).

³² M. L. Cohen and Y. W. Tsang, in *The Physics of Semimetals and Narrow-Gap Semiconductors*, edited by D. L. Carter and R. T. Bate (Pergamon, Oxford, 1971), p. 303.

³³ O. J. Glembocki and F. H. Pollack, *Phys. Rev. Lett.* **48**, 413 (1982).

³⁴ S. Bednarek and U. Rössler, *Phys. Rev. Lett.* **48**, 1296 (1982).

³⁵ O. J. Glembocki and F. H. Pollack, *Phys. Rev. B* **25**, 7863 (1982).

³⁶ D. C. Herbert, *J. Phys. C* **6**, 2788 (1973); W. Fawcett and D. C. Herbert, *ibid.* **7**, 1641 (1974).

³⁷ S. L. Richardson, M. M. Dacorogna, F. H. Pollak, M. L. Cohen, and O. J. Glembocki, in *18th International Conference on the Physics of Semiconductors*, edited by O. Engström, (World Scientific, Singapore, 1987), Vol. 2, p. 1353.

- ³⁸ M. Kienner, H. Rakel, C. Falter, and W. Ludwig, in *Phonons 89: Proceedings of the Third International Conference on Phonon Physics and the Sixth International Conference on Phonon Scattering in Condensed Matter*, edited by S. Hunklinger, W. Ludwig, and G. Weiss (World Scientific, Singapore, 1990), Vol. 1, p. 196.
- ³⁹ S. Krishnamurthy, A. Sher, and A.-B. Chen, *Appl. Phys. Lett.* **53**, 1853 (1988).
- ⁴⁰ S. Zollner, S. Gopalan, and M. Cardona, in *Phonons 89: Proceedings of the Third International Conference on Phonon Physics and the Sixth International Conference on Phonon Scattering in Condensed Matter*, edited by S. Hunklinger, W. Ludwig, and G. Weiss (World Scientific, Singapore, 1990), Vol. 2, p. 787.
- ⁴¹ In order to simplify the notation, we develop the formalism only for normal processes, i.e., we set the reciprocal lattice vector \mathbf{G} to zero. In the actual program, *umklapp* processes were included.
- ⁴² C. Jacoboni and L. Reggiani, *Rev. Mod. Phys.* **55**, 645 (1983).
- ⁴³ L. Reggiani, in *Hot-electron transport in semiconductors*, edited by L. Reggiani (Springer, Berlin, 1985), p. 60.
- ⁴⁴ R. M. Wentzcovitch, M. Cardona, M. L. Cohen, and N. E. Christensen, *Solid State Commun.* **67**, 927 (1988).
- ⁴⁵ K. Kunc and O. H. Nielsen, *Comput. Phys. Commun.* **16**, 181 (1979); **17**, 413 (1979); O. H. Nielsen and W. Weber, *ibid.* **18**, 101 (1979).
- ⁴⁶ K. Kunc and H. Bilz, *Solid State Commun.* **19**, 1027 (1976); P. H. Borchers and K. Kunc, *J. Phys. C* **11**, 4145 (1978); D. L. Price, J. M. Rowe, and R. M. Nicklow, *Phys. Rev. B* **3**, 1268 (1971).
- ⁴⁷ G. Dolling and J. L. T. Waugh, in *Lattice Dynamics*, edited by R. F. Wallis (Pergamon, Oxford, 1965), p. 19.
- ⁴⁸ W. Weber, *Phys. Rev. B* **15**, 4789 (1977).
- ⁴⁹ K. Kunc and R. M. Martin, in *Ab Initio Calculation of Phonon Spectra*, edited by J. T. Devreese, V. E. Van Doren, and P. E. Van Camp (Plenum, New York, 1983), p. 65.
- ⁵⁰ C. Falter, W. Ludwig, and M. Seimke, in *Phonon Physics*, edited by J. Kollár, N. Kroó, N. Menyhaárd, and T. Silkós (World Scientific, Singapore, 1985), p. 962.
- ⁵¹ D. Strauch and B. Dorner, *J. Phys. C* **19**, 2853 (1986).
- ⁵² D. Strauch and B. Dorner, *J. Phys. Condensed Matter* **2**, 1457 (1990); **2**, 1475 (1990).
- ⁵³ K. Kunc and R. M. Martin, *Phys. Rev. B* **24**, 2311 (1981).
- ⁵⁴ D. Strauch, A. P. Mayer, and B. Dorner, in *Phonons 89: Proceedings of the Third International Conference on Phonon Physics and the Sixth International Conference on Phonon Scattering in Condensed Matter*, edited by S. Hunklinger, W. Ludwig, and G. Weiss (World Scientific, Singapore, 1990), Vol. 1, p. 79; *Z. Phys. Condensed Matter* **78**, 405 (1990).
- ⁵⁵ K. Kunc and P. Hagège, in *Phonon Physics*, edited by J. Kollár, N. Kroó, N. Menyhaárd, and T. Silkós (World Scientific, Singapore, 1985), p. 943.
- ⁵⁶ C. Cheng, K. Kunc, and V. Heine, *Phys. Rev. B* **39**, 5892 (1989).
- ⁵⁷ M. L. Cohen and T. K. Bergstresser, *Phys. Rev.* **141**, 789 (1966).
- ⁵⁸ J. P. Walter and M. L. Cohen, *Phys. Rev.* **183**, 763 (1969).
- ⁵⁹ S. Zollner, S. Gopalan, and M. Cardona, *Appl. Phys. Lett.* **54**, 614 (1989).
- ⁶⁰ The selection rules for IV scattering, based on recent measurements and calculations of symmetries at L and X , have been summarized in Ref. 59. A more detailed account is given in Refs. 61 and 62 for the diamond and in Refs. 63 and 64 for the zinc-blende structure.
- ⁶¹ M. Lax and J. J. Hopfield, *Phys. Rev.* **124**, 115 (1961).
- ⁶² J. L. Birman, *Phys. Rev.* **127**, 1093 (1962).
- ⁶³ C. J. Bradley and B. L. Davies, *J. Math. Phys.* **11**, 1536 (1970).
- ⁶⁴ J. L. Birman, M. Lax, and R. London, *Phys. Rev.* **145**, 620 (1966).
- ⁶⁵ P. B. Allen and M. Cardona, *Phys. Rev. B* **23**, 1495 (1981); **24**, 7479 (E) (1981); **27**, 4760 (1983); P. Lautenschlager, P. B. Allen, and M. Cardona, *ibid.* **31**, 2163 (1985).
- ⁶⁶ P. B. Allen and V. Heine, *J. Phys. C* **9**, 2305 (1976).
- ⁶⁷ N. W. Ashcroft and N. D. Mermin, *Solid State Physics* (Saunders College, Philadelphia, 1976).
- ⁶⁸ L. J. Sham, *Proc. Phys. Soc.* **78**, 895 (1961).
- ⁶⁹ W. A. Harrison, *Pseudopotentials in the Theory of Metals* (Benjamin, New York, 1966), p. 309.
- ⁷⁰ P. Lautenschlager, P. B. Allen, and M. Cardona, *Phys. Rev. B* **33**, 5501 (1986).
- ⁷¹ E. M. Conwell, *High Field Transport in Semiconductors*, *Solid State Physics Suppl.* **9** (Academic, New York, 1967), p. 149.
- ⁷² W. Fawcett, A. D. Boardman, and S. Swain, *J. Phys. Chem. Solids* **31**, 1963 (1970).
- ⁷³ G. L. Bir and G. E. Pikus, *Symmetry and Strain-Induced Effects in Semiconductors* (Wiley, New York, 1974).
- ⁷⁴ J. Menendez and M. Cardona, *Phys. Rev. B* **31**, 3696 (1985).
- ⁷⁵ See *Landolt-Börnstein, Numerical Data and Functional Relationships in Science and Technology*, edited by O. Madelung, (Springer, Berlin, 1987), Vol. 22, for a compilation of experimental data.
- ⁷⁶ M. Cardona and S. Zollner, in *Properties of GaAs* (INSPEC data base, 1990).
- ⁷⁷ D. N. Mirlin (private communication).
- ⁷⁸ P. B. Allen, *Phys. Status Solidi B* **120**, 529 (1983).
- ⁷⁹ W. B. Wang, N. Ockman, M. Yan, and R. R. Alfano, *Solid-State Electron.* **32**, 1337 (1989); *SPIE Conf. Proc.* **1282** (to be published).
- ⁸⁰ S. Zollner, S. Gopalan, and M. Cardona, *SPIE Conf. Proc.* **1282** (to be published).
- ⁸¹ The pseudopotential band structures used in this work agree very well with a 16×16 $\mathbf{k} \cdot \mathbf{p}$ model for electrons in the Γ valley with energies of less than 600 meV [see T. Ruf and M. Cardona, *Phys. Rev. B* (in press)].